Integral Sliding Mode Control of Mobile Robots Based on Disturbance Observer under Saturation Conditions

Wenhui Zhang, Xiaochen Huang, Zheng Fang, Yi Zhao, Zhangping You

Abstract: **This paper presents an adaptive sliding mode control method for mobile robots under the saturation conditions of speed and torque. Under the condition of complex terrain and uncertain external disturbance, the kinematic model is constructed by combining Lyapunov stability theory and Barbalat extended lemma, and the control law satisfying the velocity constraint is designed. In order to solve the problem of decreasing control performance caused by torque saturation, an auxiliary dynamic system is proposed to dynamically adjust the torque output to avoid control signal failure by solving the torque difference between the limited and the ideal and combining with the tracking error parameters. Finally, considering the external disturbance of the mobile robot, an adaptive disturbance observer is proposed according to the influence mechanism of the external disturbance on the dynamic model, so that the system can estimate the external disturbance in real time, and enhance the robustness and adaptability of the control. Simulation results show that this method can effectively reduce the trajectory tracking error and ensure the stability and accuracy of the system in complex environment.**

Keywords: **Wheeled mobile robots; Saturation; Disturbance observer; Sliding mode control**

I. INTRODUCTION

In the process of autonomous navigation and control of mobile robots, the saturation of speed and torque is a key problem, which will significantly affect the performance and stability of the control system[1-4]. In particular, the topography of the planet's surface is complex and varied, including steep slopes, pits, sand, rocks and so on. Saturation of speed and torque can limit the robot's ability to maneuver in these complex terrains, while operating at saturation can lead to increased wear on motors or mechanical components. This puts forward higher requirements for high-precision trajectory tracking and robustness of mobile robots. However, the traditional control methods usually ignore the limit of input saturation, which makes the system difficult to meet the expected performance indicators in practical applications.

In recent years, domestic and foreign scholars have made some explorations and achieved some research results in response to such working conditions [4-7]. Chen et al. [8] proposed a tracking control method based on first-order filters, which designed the controller under the constraints of speed and torque. However, it is assumed that the inertia matrix and damping coefficient are constant, but these parameters may change in actual operation due to the change of speed, acceleration, load and other factors. Chen et al. [9] proposed a control method combining adaptive neural network and barrier Lyapunov function to effectively deal with velocity constraints and system uncertainties and improve trajectory tracking accuracy, but its dynamic model did not consider the problem of moment limitation. Bla Z. et al. [10] proposed a high order kinematic model to address the discontinuity problem of Angle errors in traditional models. Du et al. [11] proposed and designed an auxiliary dynamic system to ensure that the control signal would not exceed the physical limit of the propulsion system, so as to prevent system performance degradation or instability. Shojaei et al. [12] proposed a neural adaptive robust output feedback controller, which uses neural network and adaptive robust control technology to deal with the uncertainty and unknown parameters of the system, and reduces the influence of actuator saturation through the saturation characteristics of hyper hyperbolic tangent function. Shojaei et al. [13] studied the trajectory tracking control problem of internally damped Euler-Lagrange (EL) systems with input saturation constraints. An adaptive controller based on output feedback is proposed, which uses generalized saturation function to reduce the risk of actuator saturation effectively. The semi-global uniform final boundness of the system is proved by Lyapunov stability analysis. The research results of the appeal provide a way to consider the high precision control under the conditions of speed and moment limitation.

Considering the complexity of mobile robot working environment, a sliding mode control method based on adaptive disturbance observer is proposed to solve the mobile robot control problem with modeling error, external disturbance and input-output limitation. The main contributions of this paper are as follows:

(i) By combining Lyapunov stability theory and Barbalat extended lemma to determine the parameter selection conditions, the control law satisfying the velocity and acceleration constraints is designed.

(ii) Aiming at the nonlinear saturation problem of the output torque, an auxiliary dynamic system is designed to

Manuscript received January 1, 2025; revised March 28, 2025.

This work was supported by the National Natural Science Foundation of China (61772247), the industry-Academia-Research Cooperation Projects of Jiangsu Province (BY2022651), the Key Foundation projects of Lishui (2023LTH03), Zhejiang Qianlin Sewing Equipment Co., Ltd. Doctoral Innovation Station, Discipline Construction Project of Lishui University (Discipline Fund Name: Mechanical Engineering).

W. H Zhang is a professor at Nanjing Xiaozhuang University, Nanjing 211171, P. R. China (e-mail: hit_zwh@126.com).

X. C Huang is a postgraduate student at Zhejiang Sci-Tech University, Hangzhou 310018, P. R. China (email: hxc1249006389@163.com).

Z Fang is an engineer at State Grid Zhejiang Lishui Power Supply Company, Lishui 323000, P. R. China (e-mail: 76896419@qq.com).

Y Zhao is a professor at Lishui Key Laboratory of High Power Density Intelligent Drive System and Zhejiang Qianlin Sewing Equipment Co., Ltd., Lishui 323000, P. R. China (e-mail: 9826579@qq.com).

Z. P You is a professor at Lishui University, Lishui 323000, P. R. China (corresponding author to provide phone: +86-15925725686; e-mail: 44536388@qq.com).

dynamically compensate and adjust when the physical limit is about to be reached, so as to avoid the failure or performance degradation caused by excessive control signal. (iii) This paper designs an adaptive disturbance observer to quickly estimate external disturbances acting on mobile robots, ensuring the stability and robustness of trajectory tracking in complex environments.

II. Kinematic and Dynamic Modeling of Wheeled Mobile Robot

Robot kinematics modeling is the basis of robot motion control, and the accuracy of the model directly determines the accuracy of the control. However, it is often difficult to achieve the desired performance index when the trajectory tracking is only carried out at the kinematic level[14-17]. Therefore, this paper considers the combination of kinematics and dynamics to establish the functional relationship between torque and velocity.

Ideally, the Lagrangian formal dynamic equation of WMR is generally expressed as:

$$M(q)\ddot{q}+V(q,\dot{q})\dot{q}+G(q)+\tau_d+A^T(q)\lambda=B(q)\tau \tag{1}$$

Where: $M(q)$ represents the inertia matrix, $V(q,\dot{q})$ denotes the Coriolis matrix, $G(q)$ stands for the gravitational term, $B(q)$ signifies the transformation matrix, $A^T(q)$ is the matrix associated with constraints, τ represents the torque term, and λ denotes the Lagrangian operator.

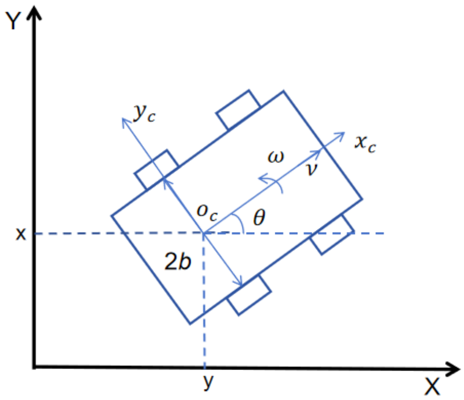

Fig. 1 Wheeled mobile robot movement diagram

Fig.1 is a schematic diagram of a wheeled mobile robot whose driving wheel center coincides with the robot's center of gravity; XOY represents the inertial coordinate system, while $x_c o_c y_c$ denotes the robot coordinate system. $q=[x,y,\theta]^T$ represents the position and orientation angle of the robot in the inertial coordinate system.

The transformation of the velocity of the robot's center of mass from the inertial coordinate system to the robot coordinate system can be calculated as follows:

$$\begin{bmatrix}\dot{x}\\ \dot{y}\\ \dot{\theta}\end{bmatrix}=\begin{bmatrix}\cos\theta & 0\\ \sin\theta & 0\\ 0 & 1\end{bmatrix}\begin{bmatrix}v\\ w\end{bmatrix} \tag{2}$$

v is the linear velocity of the robot, and w is the angular velocity of the robot. For ease of calculation, let the transformation matrix be:

$$S(q)=\begin{bmatrix}\cos\theta & 0\\ \sin\theta & 0\\ 0 & 1\end{bmatrix} \tag{3}$$

By differentiating equation (1) with respect to time, substituting equation (2) and multiplying by $S^T(q)$, the constraint matrix $A^T(q)=\begin{bmatrix}-\sin\theta & \cos\theta & 0\end{bmatrix}$ can be eliminated because $S^T(q)A^T(q)=0$. Therefore, the dynamic model of WMR obtained is as follows:

$$(S^TB)^{-1}S^TMS\dot{v}+(S^TB)^{-1}S^T(M\dot{S}+VS)v+\tau_d=\tau \tag{4}$$

$\tau_d=[\tau_{dl}\quad \tau_{dr}]^T$ represents the external disturbance acting on the WMR, which can be rewritten by a properly defined model as:

$$\bar{M}(q)\dot{v}+\bar{V}(q)v+\tau_d=\tau \tag{5}$$

In formula (5), $\bar{M}(q)=(S^TB)^{-1}S^TMS$, $\bar{V}(q)=(S^TB)^{-1}S^T(M\dot{S}+VS)$.

Note: S^TB is a constant non-singular matrix that depends on the distance between the drive wheel and the wheel radius (see Figure 1). System (4) describes the behavior of a nonholonomic system in a new set of local coordinates. Thus, the properties of the dynamics remain unchanged in the new coordinate system.

III. Kinematic Controller Based on Velocity Saturation Constraint

Design the control system as illustrated in Fig. 2.

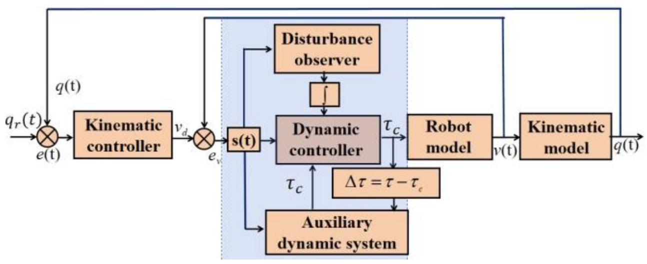

Fig. 2 Control system framework

In practical situations, excessive speed will cause the wheels of the robot to slip, and the motor will fluctuate at low speed, and the performance will decline. And too much acceleration can cause the wheel to slip or even overturn. Therefore, this paper designs the restriction conditions that meet the actual situation.

Hypothesis 1: The desired linear and angular velocities of the robot meet the following constraints:

$$\begin{cases}v_{\min}\le v\le v_{\max}\\ -w_{\min}\le w\le w_{\max}\\ |\dot{v}|\le a_v,|\dot{w}|\le a_w\end{cases} \tag{6}$$

Where, $v_{\min}$, $v_{\max}$, $w_{\min}$, $w_{\max}$, a_v and a_w are normal numbers.

Given the reference trajectory $q_d(t)=(x_d,y_d,\theta_d)^T$, the kinematic model of the expected pose can be expressed as:

$$\begin{bmatrix}\dot{x}_d\\ \dot{y}_d\\ \dot{\theta}_d\end{bmatrix}=\begin{bmatrix}\cos\theta_d & 0\\ \sin\theta_d & 0\\ 0 & 1\end{bmatrix}\begin{bmatrix}v_d\\ w_d\end{bmatrix} \tag{7}$$

Where v_d is the desired linear velocity of the robot and w_d is the desired angular velocity of the robot. The expected linear and angular velocities meet the following conditions:

$$v_{\min} \le \bar{v}_{rm} \le v_d \le \bar{v}_d \le v_{\max} \tag{8}$$

$$|w_d| \le \bar{w}_d \le w_{\max} \tag{9}$$

$$|\dot{v}_d| \le \bar{v}_{da} < a_v, |\dot{w}_d| \le \bar{w}_{da} < a_w \tag{10}$$

Where $\bar{v}_d$, $\bar{v}_{da}$, $\bar{w}_d$, and $\bar{w}_{da}$ are normal numbers.

The tracking error is:

$$e(t)=\begin{bmatrix} x_e \\ y_e \\ \theta_e \end{bmatrix}=\begin{bmatrix} \cos\theta & \sin\theta & 0 \\ -\sin\theta & \cos\theta & 0 \\ 0 & 0 & 1 \end{bmatrix}\begin{bmatrix} x_d - x \\ y_d - y \\ \theta_d - \theta \end{bmatrix} \tag{11}$$

Taking the derivative of $e(t)$ gives:

$$\dot{e}(t)=\begin{bmatrix} \dot{x}_e \\ \dot{y}_e \\ \dot{\theta}_e \end{bmatrix}=\begin{bmatrix} v_d\cos\theta_d - v + x_e\dot{\theta} \\ v_d \sin\theta + x_e\dot{\theta} \\ w_d - \dot{\theta} \end{bmatrix} \tag{12}$$

Item $v_d \cos\theta_e$ is often included in common auxiliary speed control laws, but this makes it difficult for the control law to meet the requirements of the lower limit of control speed (8). Therefore, this paper designs a new feedback function in the control law, and satisfies the restricted conditions to design the following auxiliary speed controller:

$$\begin{bmatrix} v_r \\ w_r \end{bmatrix}=\begin{bmatrix} v_d + \varphi_1 \\ w_d + \varphi_2 + \frac{\sigma_3 v_d}{\Gamma_1}\left(y_e \cos\frac{\theta_e}{2} - x_e \sin\frac{\theta_e}{2} \right) \end{bmatrix} \tag{13}$$

Where σ_3 is a constant, $\Gamma_1=\sqrt{1+x_e^2+y_e^2}$, φ_1, φ_2 is the feedback function, as follows:

$$\begin{cases} \dot{\varphi}_1 = -\varphi_1 + \frac{\sigma_1 x_e}{\Gamma_1} \\ \dot{\varphi}_2 = -\varphi_2 + \sigma_2 \sin\frac{\theta_e}{2} \end{cases} \tag{14}$$

Where σ_1 and σ_2 are positive real numbers and $\varphi_1(0)=0$ and $\varphi_2(0)=0$.

$$\begin{cases} |\varphi_1| < \sigma_1 \\ |\varphi_2| < \sigma_2 \end{cases} \tag{15}$$

According to the above formula, it can also be obtained:

$$\begin{cases} \dot{\varphi}_1 \le |\varphi_1| + \left|\frac{\sigma_1 x_e}{\Gamma_1}\right| \le 2\sigma_1 \\ \dot{\varphi}_2 = |\varphi_2| + \left|\sigma_2 \sin\frac{\theta_e}{2}|\varphi_2|\right| \le 2\sigma_2 \end{cases} \tag{16}$$

From the above formula, φ_1 is obtained, and φ_2 is bounded and continuous.

Lemma 1: If there exists a bounded function $z(t)$ that satisfies $z \to 0$ when $t \to \infty$, and $\dot{z} = -z + f(x)$, where $f(t)$ is bounded and uniformly continuous, then $\dot{z} \to 0$ and $f(t) \to 0$ when $t \to \infty$.

Select the Lyapunov function as:

$$V=\sqrt{1+x_e^2+y_e^2}-1+k_1\left(1-\cos\frac{\theta_e}{2}\right)+k_2\varphi_1^2+k_3\varphi_2^2 \tag{17}$$

Differentiating the above equation and substituting equations (12) and (13) into it yields:

$$\begin{aligned}
\dot{V} &= \frac{x_e\dot{x}_e + y_e\dot{y}_e}{\Gamma_1} + \frac{k_1}{2}\dot{\theta}_e \sin\frac{\theta_e}{2} + 2k_2\varphi_1\dot{\varphi}_1 + 2k_3\varphi_2\dot{\varphi}_2 \\
&= \frac{1}{\Gamma_1}\left[v_d x_e(\cos\theta_e - 1) - x_e\varphi_1 + v_d y_e \sin\theta_e \right] \\
&\quad -\frac{k_1}{2}\sin\frac{\theta_e}{2}\left[\varphi_2 + \frac{\sigma_3 v_d}{\Gamma_1}\left(y_e\cos\frac{\theta_e}{2} - x_e \sin\frac{\theta_e}{2} \right) \right] \\
&\quad -2k_2\varphi_1^2 + \frac{2k_2\sigma_1 x_e \varphi_1}{\Gamma_1} - 2k_3\varphi_2^2 + 2k_3\sigma_2 \sin\frac{\theta_e}{2}\varphi_2 \\
&= \frac{1}{\Gamma_1}\left[v_d x_e(\cos\theta_e - 1) + v_d y_e \sin\theta_e \right. \\
&\quad \left. -\frac{k_1\sigma_3}{4} v_d \left(x_e(\cos\theta_e - 1) - y_e \sin\theta_e \right) \right] \\
&\quad + \frac{x_e\varphi_1}{\Gamma_1}(2k_2\sigma_1 - 1) + \sin\frac{\theta_e}{2}\varphi_2\left(2k_3\sigma_2 - \frac{k_1}{2} \right) \\
&\quad -2k_2\varphi_1^2 - 2k_3\varphi_2^2
\end{aligned} \tag{18}$$

If the following conditions are met, then $V=0$.

$$\begin{cases} 2k_2\sigma_1 = 1 \\ 2k_3\sigma_2 = \frac{k_1}{2} \\ k_1\sigma_3 = 4 \end{cases} \tag{19}$$

Since $\dot{V} \le 0$ and $V(t, x_e(t), y_e(t), \theta_e(t))$ is positive definite, it follows that $V(t, x_e(t), y_e(t), \theta_e(t))$ is uniformly bounded, and thus the errors x_e, y_e and θ_e are uniformly bounded. Since $\varphi_1, \varphi_2, \dot{\varphi}_1$ and $\dot{\varphi}_2$ are bounded, $\dot{V}$ and $\ddot{V} = -4k_2\varphi_1\dot{\varphi}_1 - 4k_3\varphi_2\dot{\varphi}_2$ are also bounded. According to Barbalat's lemma, $\dot{V} \to 0$ when $t \to \infty$, that is, $\varphi_1 \to 0$ and $\varphi_2 \to 0$ when $t \to \infty$. According to lemma 1 and equation (14), x_e and $\sin\frac{\theta_e}{2}$ converge to zero.

According to equation (13), it can be obtained:

$$\dot{\theta}_e = \varphi_2 + \frac{\sigma_3 v_d}{\Gamma_1}\left(y_e \cos\frac{\theta_e}{2} - x_e \sin\frac{\theta_e}{2} \right) \tag{20}$$

Obviously $\dot{\theta}_e$ is uniformly continuous. Since $\varphi_2 \to 0$ and $\sin\frac{\theta_e}{2} \to 0$ have been proved above, according to Barbalat's lemma, $\dot{\theta}_e \to 0$ when $t \to \infty$, that is, $\varphi_2 + \frac{\sigma_3 v_d}{\Gamma_1}\left(y_e\cos\frac{\theta_e}{2} - x_e \sin\frac{\theta_e}{2} \right) \to 0$, so y_e can converge to zero. Stability proved complete. Finally, the hypothesis condition under velocity constraint is proved. According to equations (13) and (15).

$$\begin{cases} v \le |v_d| + |\varphi_2| \le \bar{v}_d + \sigma_1 + \frac{\sigma_3 v_d}{\Gamma_1}\left(y_e \cos\frac{\theta_e}{2} - x_e \sin\frac{\theta_e}{2} \right) \\ v \ge |v_{dm}| - |\varphi_1| \ge \bar{v}_{dm} - \sigma_1 \\ w \le |w_d| + |\varphi_2| + \left| \frac{\sigma_3 v_d}{\Gamma_1}\left(y_e \cos\frac{\theta_e}{2} - x_e \sin\frac{\theta_e}{2} \right) \right| \\ \quad \le \bar{w}_d + \sigma_2 + \sigma_3 v_d \end{cases} \tag{21}$$

According to equation (20) :

$$\dot{\theta}_e = |\varphi_2| + \left|\frac{\sigma_3 v_d}{\Gamma_1}\left(y_e \cos\frac{\theta_e}{2} - x_e \sin\frac{\theta_e}{2}\right)\right| \le \sigma_2 + \sigma_3 \bar{v}_d \quad (22)$$

and

$$d\left[\frac{1}{\Gamma_1}\left(y_e \cos\frac{\theta_e}{2} - x_e \sin\frac{\theta_e}{2}\right)\right]/dt$$
$$= \frac{\dot{y}_e \cos\frac{\theta_e}{2} - \frac{1}{2}\dot{\theta}_e y_e \sin\frac{\theta_e}{2} - \dot{x}_e \sin\frac{\theta_e}{2} - \frac{1}{2}\dot{\theta}_e x_e \cos\frac{\theta_e}{2}}{\Gamma_1}$$
$$- \frac{\left(y_e \cos\frac{\theta_e}{2} - x_e \sin\frac{\theta_e}{2}\right)\left(\dot{x}_e x_e + \dot{y}_e y_e\right)}{\Gamma_1^3}$$
$$\le \left|\frac{\left(v_d \sin\theta_e - w x_e\right)\cos\frac{\theta_e}{2} - \left(v_d \cos\theta_e - w y_e - v\right)\sin\frac{\theta_e}{2}}{\Gamma_1}\right.$$
$$\left.\frac{-\frac{1}{2}\dot{\theta}_e\sqrt{x_e^2 + y_e^2}\cos\left(\frac{\theta_e}{2} + \phi\right)}{\Gamma_1}\right|$$
$$- \frac{\left(y_e \cos\frac{\theta_e}{2} - x_e \sin\frac{\theta_e}{2}\right)\left(v_d x_e \cos\theta_e\right.}{\Gamma_1^3}$$
$$\frac{\left.-v_d x_e - x_e \varphi_1 + y_e v_d \sin\theta_e\right)}{\Gamma_1^3}$$
$$\le 7\bar{v}_d + 3\sigma_1 + 3\sigma_2 + 3\sigma_3 \bar{v}_d + \bar{w}_d \quad (23)$$

Taking the derivative of v_r and w_r separately gives:

$$\begin{cases} \dot{v}_r = \dot{v}_d + \dot{\varphi}_1 \le \bar{v}_{da} + 2\sigma_1 \\ \dot{w}_r = \dot{w}_d + \dot{\varphi}_2 + \sigma_3 v_d d\left[\frac{1}{\Gamma_1}\left(y_e \cos\frac{\theta_e}{2} - x_e \sin\frac{\theta_e}{2}\right)\right]/dt \\ \quad \le \bar{w}_{da} + 7\bar{v}_d + 3\sigma_1 + 5\sigma_2 + 3\sigma_3 \bar{v}_d + \bar{w}_d \end{cases} \quad (24)$$

According to the above design parameters to meet the conditions:

$$\begin{cases} \bar{v}_d + \sigma_1 \le v_{\max} \\ \bar{v}_{dm} - \sigma_1 \ge v_{\min} \\ \bar{w}_d + \sigma_2 + \sigma_3 v_d \le \bar{w}_{\max} \\ \bar{v}_{da} + 2\sigma_1 \le a_v \\ \bar{w}_{da} + 7\bar{v}_d + 3\sigma_1 + 5\sigma_2 + 3\sigma_3 \bar{v}_d + \bar{w}_d \le a_w \end{cases} \quad (25)$$

By selecting reasonable parameters σ_1, σ_2 and σ_3 according to equation (10), condition (25) and $\dot{V} \le 0$ can be satisfied. Therefore, both the speed and acceleration limits can be satisfied, and the tracking error $e(t)$ can be asymptotically converged to zero.

IV. Dynamic Controller Based on Torque Saturation Constraint

A. Integral sliding mode control

In order to improve the dynamic adaptability of WMR to uncertain disturbance, a robot dynamic controller is designed in this paper. First, the auxiliary velocity tracking error vector $e_v = \nu - \nu_r$, where $\nu_r = \begin{bmatrix} v_r & w_r \end{bmatrix}^T$, is defined. On this basis, the integral sliding mode surface is designed:

$$s(t) = ce_v + \int_0^t e_v dt \quad (26)$$

Where $c = \begin{bmatrix} c_1 & c_2 \end{bmatrix}$, c_1 and c_2 are normal numbers. If the perturbation of the system is known to be $\tau_d = \begin{bmatrix} \tau_{d1} & \tau_{d2} \end{bmatrix}^T$, the WMR dynamics equation can be expressed in terms of the sliding mode surface as:

$$\bar{M}\dot{s} = c\bar{M}e_v - \bar{M}\dot{\nu}_r + \tau - \bar{V}_m \nu - \tau_d \quad (27)$$

Based on this assumption of known system perturbations, the design control law is:

$$\tau = \bar{M}\dot{\nu}_r - c\bar{M}e_v + \bar{V}_m \nu + \tau_d - \bar{M}\left[\lambda_1 \tanh(ks) + \lambda_2 s\right] \quad (28)$$

Where λ_1 and λ_2 are normal numbers. The hyperbolic tangent function $\tanh(ks)$ was chosen because, as a continuous function, it has better buffeting suppression properties than the sign function, where $k > 0$ is used to determine the step length time.

Lemma 2: For the dynamic model (5) of wheeled mobile robot, when the external disturbance τ_d is known, the integral sliding mode surface formula (26) and the total controller formula (28) can ensure the global asymptotic stability of the control system.

The stability analysis is as follows[27-35]:

Select the Lyapunov function as:

$$V_1 = \frac{1}{2}s^T s \quad (29)$$

Obviously $V_1 > 0$. The derivative of time is:

$$\begin{aligned} \dot{V}_1 &= s^T \dot{s} \\ &= s^T\left(ce_v - \dot{\nu}_r + \bar{M}^{-1}\tau - \bar{M}^{-1}\bar{V}_m \nu - \bar{M}^{-1}\tau_d\right) \end{aligned} \quad (30)$$

Substituting equation (28) into equation (30) yields:

$$\dot{V}_1 = -\lambda_1 s^T \tanh(ks) - \lambda_2 s^T s \quad (31)$$

Obviously, $\dot{V}_1 \le 0$. LaSalle theorem[18] is used to make the tracking error converge to zero globally.

B. Adaptive control based on disturbance observer

The external interference to WMR, such as sensor noise and uncertain friction force, will cause the system variables related to the sliding mode surface to produce severe buffeting, which makes the controller stability cannot be guaranteed. In complex unstructured environments, uncertain perturbations must be unknown. Therefore, the controller with the preset disturbance value is not satisfied with the actual WMR control. However, the rate of change of interference is much slower than the processing speed of the computer. Therefore, an adaptive disturbance observer can be introduced to estimate the uncertain disturbance[19-25].

The estimated disturbance vector is expressed as $\hat{\tau}_d = \begin{bmatrix} \hat{\tau}_{d1} & \hat{\tau}_{d2} \end{bmatrix}^T$, and the disturbance estimation error is $\tilde{\tau}_d = \hat{\tau}_d - \tau_d$. Since the rate of change of the disturbance is slower due to the faster processing speed of the computer, $\dot{\tilde{\tau}}_d = \dot{\hat{\tau}}_d$. Therefore, the original control law can be extended by introducing adaptive disturbance estimation to:

$$\tau = \bar{M}\dot{\nu}_r - c\bar{M}e_v + \bar{V}_m \nu + \hat{\tau}_d - \bar{M}\left[\lambda_1 \tanh(ks) + \lambda_2 s\right] \quad (32)$$

$$\dot{\hat{\tau}}_d = -\eta s^T \bar{M}^{-1} \quad (33)$$

Where $\eta > 0$. η determines the time of convergence.

As shown in Figure 3, in practical applications, due to the physical limitations of the motor, the controlling force and torque are affected by saturation nonlinearity, which can be described as follows:

$$\tau=\begin{cases}\tau_{\max} & \tau_c>\tau_{\max}\\ \tau_c & -\tau_{\max}\le\tau_c\le\tau_{\max}\\ -\tau_{\max} & \tau_c<-\tau_{\max}\end{cases} \tag{34}$$

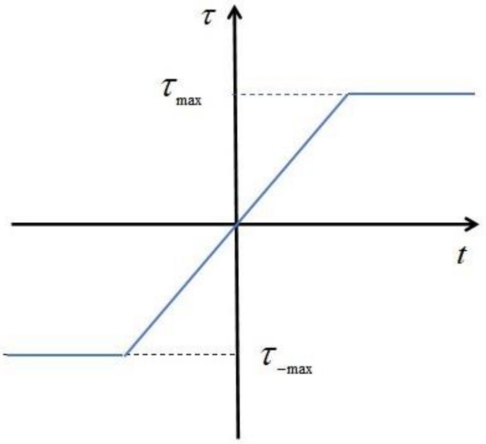

Fig.3 Torque saturation diagram

In order to prevent input saturation, this paper constructs the following auxiliary dynamic system:

$$\dot{\varepsilon}=\begin{cases}-K_\varepsilon\varepsilon-\dfrac{\sum_{i=1}^{2}\left|s_i\Delta\tau_i\right|+\dfrac{1}{2}\Delta\tau^T\Delta\tau}{\|\varepsilon\|}\varepsilon+\Delta\tau, & \|\varepsilon\|\ge\sigma\\ 0 & \|\varepsilon\|<\sigma\end{cases} \tag{35}$$

Where $\varepsilon=\left[\varepsilon_1 \quad \varepsilon_2\right]^T$ is the state vector of the auxiliary power system, $\Delta\tau=\tau-\tau_c$, $K_\varepsilon=K_\varepsilon{}^T\in R^{2\times2}$ is a positive definite matrix, and $\sigma>0$ is a smaller normal number. The auxiliary dynamic system (35) avoids the singularity problem of $\dot{\varepsilon}=0$ when $\|\varepsilon\|<\sigma$. Therefore, the control law is expanded to:

$$\begin{aligned}\tau_c&=\bar{M}\dot{v}_r-c\bar{M}e_v+\bar{V}_m v-\bar{M}K_s\varepsilon+\hat{\tau}_d\\&\quad-\bar{M}\left[\lambda_1\tanh\left(ks\right)+\lambda_2 s\right]\end{aligned} \tag{36}$$

Lemma 3: For the dynamic model (5) of wheeled mobile robot, when the external disturbance τ_d is unknown, the integral sliding mode surface formula (24), adaptive interference observer (33) and total controller formula (32) are adopted to achieve global asymptotic stability of the control system.

Select the Lyapunov function as:

$$V_2=\frac{1}{2}s^Ts+\frac{1}{2\mu}\tilde{\tau}_d^T\tilde{\tau}_d+\frac{1}{2}\varepsilon^T\varepsilon \tag{37}$$

Obviously $V_2>0$. The derivative of time is:

$$\dot{V}_2=s^T\dot{s}+\frac{1}{\mu}\tilde{\tau}_d^T\dot{\tilde{\tau}}_d+\varepsilon^T\dot{\varepsilon} \tag{38}$$

Considering the auxiliary dynamic system to prevent the moment saturation, the stability analysis of the control system is divided into two cases. The first case is when $\|\varepsilon\|\ge\sigma$, according to equation (35) and young's inequality[26]:

$$\begin{aligned}\varepsilon^T\dot{\varepsilon}&=-\varepsilon^TK_\varepsilon\varepsilon-\sum_{i=1}^{2}\left|s_i\Delta\tau_i\right|-\frac{1}{2}\Delta\tau^T\Delta\tau+\varepsilon^T\Delta\tau\\&\le-\varepsilon^TK_\varepsilon\varepsilon-\sum_{i=1}^{2}\left|s_i\Delta\tau_i\right|+\frac{1}{2}\varepsilon^T\varepsilon\end{aligned} \tag{39}$$

Substituting equations (33), (36), and (39) into equations (38) yields:

$$\begin{aligned}\dot{V}_2&=s^T\left(ce_v-\dot{v}_r+\bar{M}^{-1}\tau_c-\bar{M}^{-1}\bar{V}_m v\right.\\&\quad\left.-\bar{M}^{-1}\hat{\tau}_d+\bar{M}^{-1}\tilde{\tau}_d\right)\dot{s}+\frac{1}{\mu}\tilde{\tau}_d^T\dot{\hat{\tau}}_d+\varepsilon^T\dot{\varepsilon}\\&=s^T\left(ce_v-\dot{v}_r+\bar{M}^{-1}\left(\tau_c-\bar{V}_m v-\hat{\tau}_d\right)\right)\\&\quad+\left(s^T\bar{M}^{-1}+\frac{1}{\mu}\dot{\hat{\tau}}_d\right)\tilde{\tau}_d^T+\varepsilon^T\dot{\varepsilon}\\&=-\lambda_1 s^T\tanh\left(ks\right)-\lambda_2 s^Ts-s^TK_s\varepsilon+\varepsilon^T\dot{\varepsilon}\\&\le-\lambda_1 s^T\tanh\left(ks\right)-\lambda_2 s^Ts-\frac{1}{2}s^Ts-\frac{1}{2}\varepsilon^TK_s^TK_s\varepsilon\\&\quad-\varepsilon^TK_\varepsilon\varepsilon-\sum_{i=1}^{2}\left|s_i\Delta\tau_i\right|+\frac{1}{2}\varepsilon^T\varepsilon\\&\le-\lambda_1 s^T\tanh\left(ks\right)-\left(\frac{1}{2}+\lambda_2\right)s^Ts\\&\quad-\left(K_\varepsilon+\frac{1}{2}K_s^TK-\frac{1}{2}\right)\varepsilon^T\varepsilon\end{aligned} \tag{40}$$

The second case is when $\|\varepsilon\|<\sigma$, then:

$$\varepsilon^T\dot{\varepsilon}=0 \tag{41}$$

Substituting equations (33), (36), and (41) into equations (38) yields:

$$\begin{aligned}\dot{V}_2&\le-\lambda_1 s^T\tanh\left(ks\right)-\lambda_2 s^Ts-\frac{1}{2}s^Ts-\frac{1}{2}\varepsilon^TK_s^TK_s\varepsilon\\&\le-\lambda_1 s^T\tanh\left(ks\right)-\left(\frac{1}{2}+\lambda_2\right)s^Ts-\frac{1}{2}\varepsilon^TK_s^TK_s\varepsilon\end{aligned} \tag{42}$$

If the design parameters K_ε , K_s and λ_2 meet the following conditions, $\dot{V}_2\le0$.

$$K_\varepsilon+\frac{1}{2}K_s^TK_s>\frac{1}{2} \tag{43}$$

V. SIMULATION EXPERIMENT

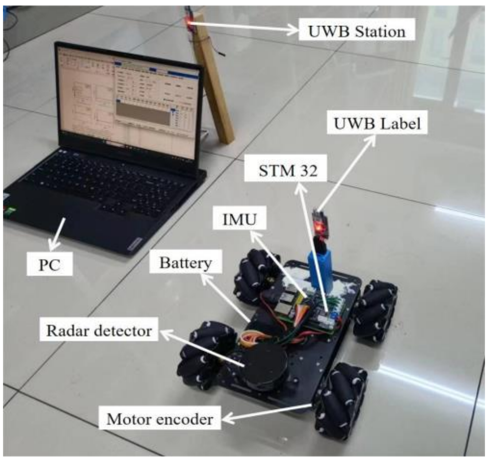

Fig. 4 WMR platform

In this section, this paper conducts simulation experiments on the mobile robot platform subject to velocity constraint/torque saturation constraint. Figure 4 is shown as the controlled object verified by the experiment to prove the effectiveness of the proposed scheme. Formula (5) is used as the dynamic mathematical model.

The robot system parameters are the total weight m=10kg, the total moment of inertia of the robot $I = 7.884 kg \cdot m^2$, the radius of the wheel r=0.05, and the distance between the wheel and the center of the two wheels b=0.15m.

The parametric equation $\begin{cases} x_d = \cos t \\ y_d = \sin t \end{cases} (t \geq 0)$ for the expected trajectory is a circular trajectory. The design parameters of the controller in this paper are $k_1 = 0.9, k_2 = 0.2, k_3 = 1.4, c_1 = c_2 = 7, K_\xi = diag(5,5)$, and the external disturbance $\tau_d = [0.1\cos t, 0.1\sin t]$. At the same time, in order to make the disturbance irregular, the pose disturbance $\tau_d' = [0.1\cos t, 0.1, 0.1\sin t]$ is added. The initial pose is $q = [1.5 \quad -0.5 \quad 0]^T$, the expected linear velocity is $v_d = 0.6 m/s$, and the expected angular velocity is $v_d = 0.3 rad/s$.

The tracking situation of a given expected circular trajectory is shown in Fig.5. It can be seen from Fig.6 of position and pose tracking error that the error convergence accuracy can basically be stabilized at about 0.1 meters. The curves of the expected speed, virtual speed and actual speed are shown in Fig.7, from which it can be seen that the actual speed successfully tracks the expected linear speed and meets the condition that the speed limit is up to 1m/s. Fig.8 shows the tracking error curve of the velocity, because the existence of disturbance makes the velocity fluctuate, but the control system has controlled the linear velocity tracking error within 0.1m/s, and the angular velocity tracking error within 0.02rad/s.

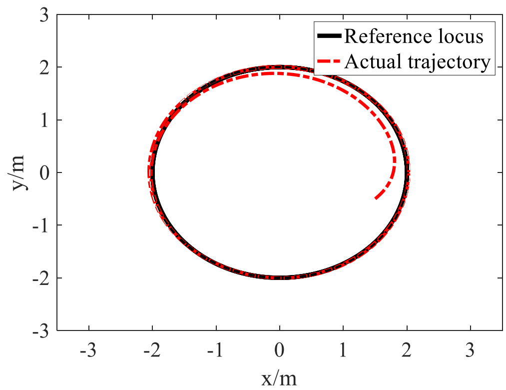

Fig.5 Circular trajectory tracking curve

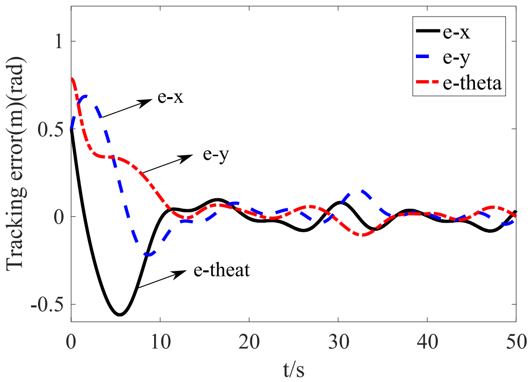

Fig.6 Pose tracking error

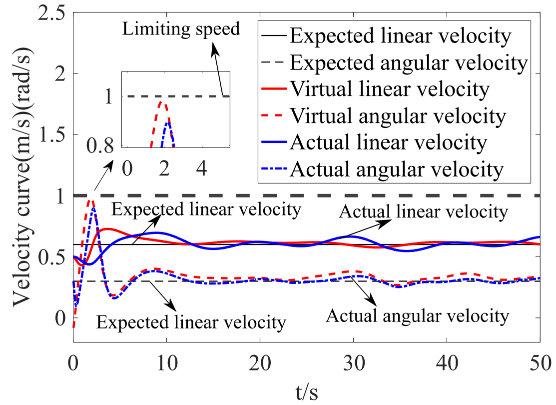

Fig.7 Velocity curve

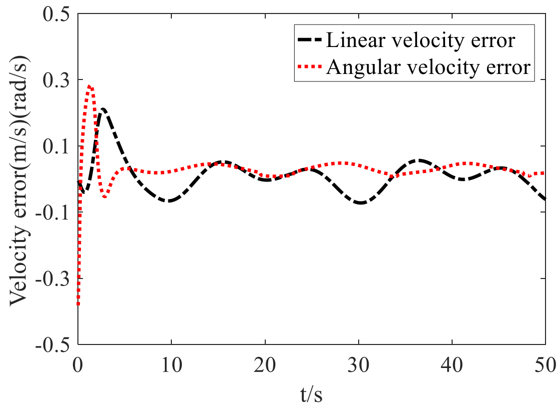

Fig. 8 Velocity error curve

Fig.9 shows the torque control input curve of the left and right wheels, with a maximum torque limit of 0.7N. As can be seen from the figure, under the action of the auxiliary power system, the torque of the right wheel does not exceed the maximum torque limit. Fig.10 shows the torque curve of the control system when the auxiliary power system is on and off. Since the torque of the left wheel does not tend to approach the maximum torque, only the torque comparison diagram of the right wheel is given. As can be seen from the figure, after the auxiliary power system is closed, the torque of the right wheel obviously reaches the maximum limit torque, and the torque curve is not smooth, which will further damage the motor. Fig.11 and Fig.12 show the disturbance estimation of left wheel torque and right wheel torque by the disturbance observer respectively. As can be seen from the figure, the disturbance observer can quickly track the disturbance within 2 seconds, and the observation error is within 0.01N.

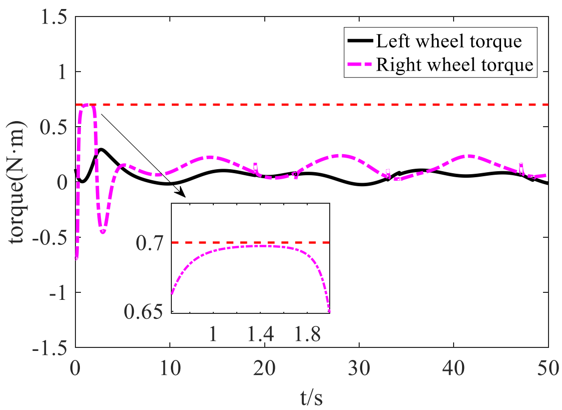

Fig. 9 Left and right wheel control torque

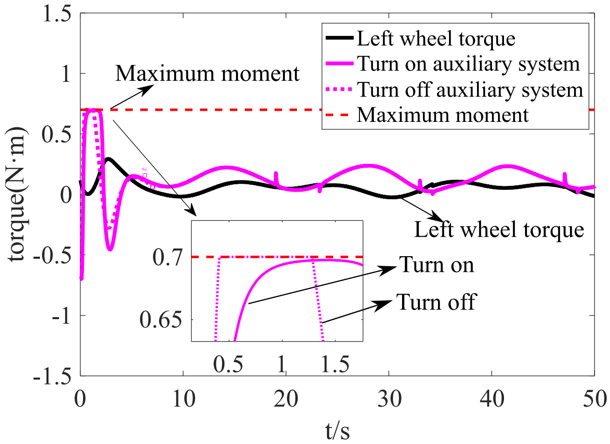

Fig.10 Torque comparison with and without auxiliary dynamic systems

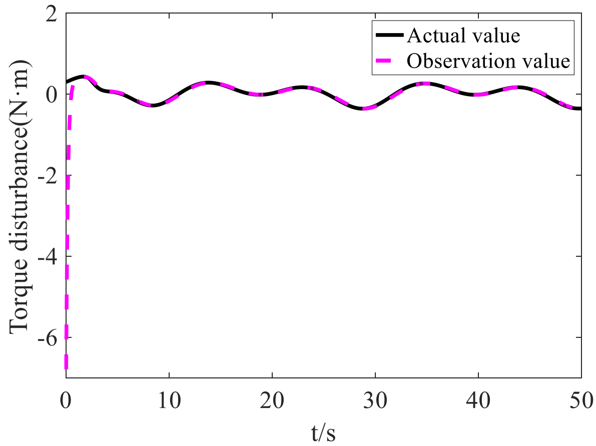

Fig.11 Disturbance estimation of left wheel torque

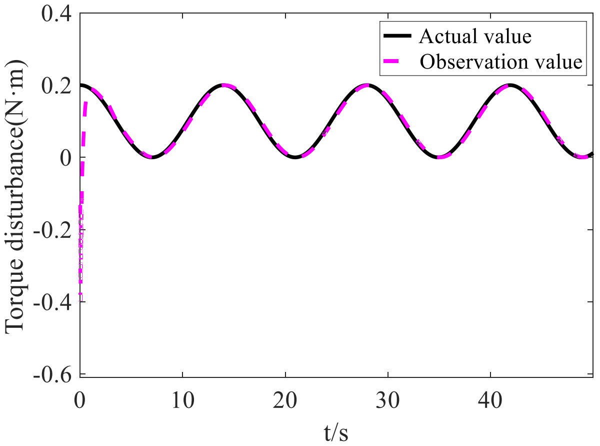

Fig.12 Disturbance estimation of right wheel torque

Fig.13 shows the effect of circular trajectory tracking without observer. It can be clearly seen that the tracking effect of the control system without feedback from the disturbance observer is poor. Fig 14-16 compares the pose tracking errors of the X axis, Y axis, and Angle of the closed and open disturbance observer. It can be seen from the figure that without the feedback value of the disturbance observer, the tracking error is greatly affected by the disturbance, and the tracking effect becomes worse.

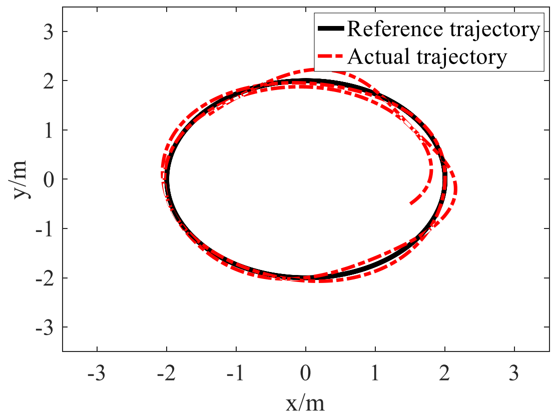

Fig.13 Observerless circular trajectory tracking

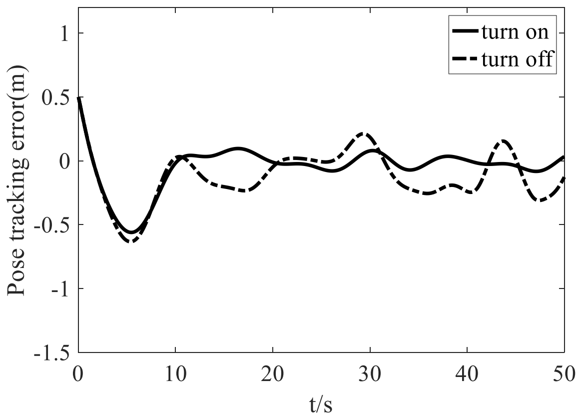

Fig.14 X-axis error comparison with or without observer

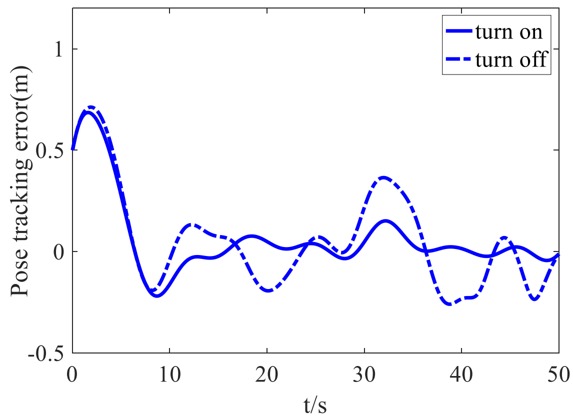

Fig. 15 Y-axis error comparison with or without observer

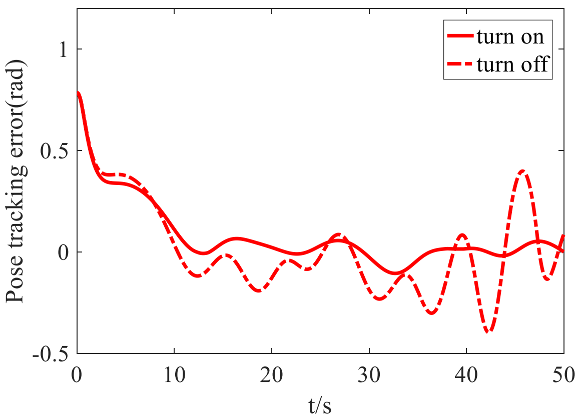

Fig.16 Comparison of Angle error with or without observer

VI. CONCLUSION

A disturbance observer based adaptive sliding mode control method is proposed to address the stability control problem of wheeled mobile robots under speed constraints/torque saturation constraints, while considering uncertainties such as modeling errors and external disturbances. A kinematic model was established, taking into account boundary conditions, and a kinematic control law was designed. A sliding mode controller based on a dynamic torque regulator was designed to address modeling errors and torque saturation issues. An adaptive disturbance observer was also designed to achieve real-time estimation of external disturbance signals. Experimental results further verify the effectiveness of the proposed method. The effectiveness of the proposed algorithm has been verified through comparative experiments, and the control algorithm with disturbance observer has higher control accuracy.

REFERENCE

[1] W Zhang, X Ye and X Ji, "RBF neural network adaptive control for space robots without speed feedback signal, "Transactions of the Japan Society for Aeronautical and Space Sciences, vol.56, no.6, pp. 317-322, 2013

[2] L Jiang, W Zhang, J Shen, et al. "Vibration Suppression of Flexible Joints Space Robot based on Neural Network, "IAENG International Journal of Applied Mathematics, vol.52, no.4, pp. 776-783, 2022

[3] Z You, W Zhang, J Shen, et al. "Adaptive neural network vibration suppression control of flexible joints space manipulator based on H∞ theory, "Journal of Vibroengineering, vol.25, no.3, pp. 492-505, 2023

[4] W Zhang, F Gao, J Huang, et al. "Global Prescribed-Time Stabilization for a Class of Uncertain Feedforward Nonlinear Systems, " IEEE Transactions on Circuits and Systems II: Express Briefs, vol.70, no.4, pp. 1450-1454, 2022

[5] W Zhang, X Ye and L Jiang, "Output feedback control for free-floating space robotic manipulators base on adaptive fuzzy neural network, "Aerospace Science and Technology,vol.29, no.1, pp. 135–143, 2013

[6] L Yin, W Zhang, T Zhou, et al. "Machine Health-Driven Dynamic Scheduling of Hybrid Jobs for Flexible Manufacturing Shop," International Journal of Precision Engineering and Manufacturing, vol.24, no.5, pp. 797-812, 2023

[7] W Zhang, N Qi, J MA, et al. "Neural integrated control for free-floating space robot with changing parameters," Science China: Information Science, vol.4, no.10, pp. 2091-2099, 2011

[8] X Chen, Y Jia. Simple tracking controller for unicycle-type mobile robots with velocity and torque constraints," Transactions of the Institute of Measurement and Control, vol.37, no.2, pp. 211-218, 2015

[9] Z Chen, Y Liu, W He, et al. "Adaptive-neural-network-based trajectory tracking control for a nonholonomic wheeled mobile robot with velocity constraints," IEEE Transactions on Industrial Electronics, 2020, 68(6): 5057-5067.

[10] BLAŽIČ S. "A novel trajectory-tracking control law for wheeled mobile robots. Robotics and Autonomous Systems, vol.59, no.11, pp. 1001-1007, 2011

[11] J Du, X Hu, M Krstić, et al. "Robust dynamic positioning of ships with disturbances under input saturation. Automatica," vol.73, pp. 207-214, 2016

[12] K SHOJAEI. "Neural adaptive robust output feedback control of wheeled mobile robots with saturating actuators." International Journal of Adaptive Control and Signal Processing, vol.29, no.7, pp. 855-876. 2015

[13] K Shojaei, A Chatraei. "A saturating extension of an output feedback controller for internally damped Euler-Lagrange systems," Asian Journal of Control, vol.17, no.6, pp. 2175-2187. 2015

[14] W Zhang, N Qi and H Yin, "Neural-network tracking control of space robot based on sliding-mode variable structure, "Control Theory and Applications, vol.28, no.9, pp. 1141-1144, 2011

[15] Y Hu and W Zhang, "Modeling framework for analyzing midair encounters in hybrid airspace where manned and unmanned aircraft coexist," Proceedings of the Institution of Mechanical Engineers, Part G: Journal of Aerospace Engineering, vol.233, no.15, pp. 5492-5506, 2019

[16] Y Fang, W Zhang and X Ye. "Variable Structure Control for Space Robots Based on Neural Networks," International Journal of Advanced Robotic Systems, vol.11, no.3, pp. 35-42, 2014

[17] W Zhang, Y Shang Q Sun, et al, "Finite-Time Stabilization of General Stochastic Nonlinear Systems with Application to a Liquid-Level System, "IAENG International Journal of Applied Mathematics, vol.51, no.2, pp. 295-299, 2021

[18] J P LaSalle. "Recent advances in Liapunov stability theory." SIAM Review, vol.6, no.1, pp. 1-11. 1964

[19] L Zhu, Xiaochen Huang, X Wu, et.al. "Neural Network Control of Robot under Wheel Slip Conditions based on Observer," Engineering Letters, vol.32, no.10, pp. 2041-2051. 2024

[20] Z You, D Yi, Z Fang, et.al. "Image Enhancement ANPSO Processing Technology Based on Improved Particle Swarm Optimization Algorithm,"IAENG International Journal of Computer Science, vol.51, no.11, pp. 1781-1792. 2024

[21] W Zhang, S Ding, D Yi, et.al. "Improved Sliding Mode Variable Structure Control of Robot Manipulators with Flexible Joints based on Singular Perturbation," 2023 International Conference on Telecommunications, Electronics and Informatics (ICTEI), pp. 288-291. 2023

[22] R Chen, Z You, W Zhang, "Adaptive Fuzzy Sliding Mode Control for Nonlinear Systems with Unknown Dead-zone," IAENG International Journal of Applied Mathematics.,vol.5, no.12, pp. 2588-2595, 2024

[23] W Zhang, J Shen X Ye, et al. "Error model-oriented vibration suppression control of free-floating space robot with flexible joints based on adaptive neural network,"Engineering Applications of Artificial Intelligence, vol.114, no.4, pp. 1-14, 2022

[24] X Guo, W Zhang and F Gao, "Global Prescribed-Time Stabilization of Input-Quantized Nonlinear Systems via State-Scale Transformation ," Electronics, vol.12, no.2, pp. 33-47, 2023

[25] W Zhang, H Chen and Z Wen, "Sliding Mode Control of Flexible Joint Space Robot for Unknown Target,"Aerospace Control and Applications, vol.47, no.3, pp. 49-56, 2021

[26] H J Brascamp, E H Lieb. "Best constants in Young's inequality, its converse, and its generalization to more than three functions," Advances in Mathematics, vol.20, no.2, pp. 151-173, 1976

[27] W. Zhang, H. S. Liu, X. P. Ye, et al. "Adaptive robust control for free-floating space robot Adaptive robust control for free-floating space robot with unknown uncertainty based on neural network with unknown uncertainty based on neural network," International Journal of Advanced Robotic Systems, vol.15, no.6, pp. 1-11, 2018.

[28] W.Zhang, Y.Zhu, "Control of free-floating space robotic manipulators base on neural network," International Journal of Computer Science Issues (IJCSI) , vol.9, No.6, pp. 322,2012.

[29] X.C. Huang, Z.P. You, W.H. Zhang, et al, "Stabilization control of wheeled mobile robot based on neural sliding mode under wheel slip conditions," International Journal of Dynamics and Control, vol. 13, no.2, pp.1-12, 2025.

[30] W.Zhang, Z.Wen, Y.Ye, and S.Zhou, "Structural mechanics analysis of bolt joint of rigid flexible coupling manipulator," Journal of Measurements in Engineering, vol.10, No.2, pp. 93-104,2022.

[31] W.Zhang, N.Qi, and Y.Li, "Output feedback PD control of robot manipulators dispense with model base on fuzzy-basis-function-network," Journal of National University of Defense Technology , vol.32, No.6, pp. 163-170,2010.

[32] D.J.Yi, Z.P.You, W.H. Zhang, "Image Enhancement CHPSO Processing Technology Based on Improved Particle Swarm Optimization Algorithm," IAENG International Journal of Computer Science, vol. 52, no.1, pp.130-142, 2025.

[33] W.Zhang, Y. Fang, X. Ye, "Adaptive Neural Network Robust Control for Space Robot with Uncertainty," TELKOMNIKA, vol.11, No.3, pp. 513-520, 2013.

[34] J. Ma, W. Zhang, and H. P. Zhu, "Adaptive Control for Robotic Manipulators base on RBF Neural Network," TELKOMNIKA, vol.11, no.3, pp. 521-528, 2013.

[35] W. Zhang, X. Ye, L. Jiang, and Y. Fang, "Robust control for robotic manipulators base on adaptive neural network," The Open Mechanical Engineering Journal，vol.20, no.8, pp. 497-502, 2014.